CRYSTAL GROWTH & DESIGN
2007
VOL. 7, NO. 7
1365−1372

4,4′-Dipyridyl-*N*,*N*′-dioxide Complexes of Metal-Thiocyanate/Selenocyanate: π-Stacked Molecular Rods as Three-Dimensional Support for Two-Dimensional Polymeric Sheets and Intra/Interchain S···S Interaction Dependent Architecture of the $R_2^2(8)$ Synthon Driven Assembly of One-Dimensional Polymeric Chains

Atish Dipankar Jana,[†] Subal Chandra Manna,[‡] Georgina M. Rosair,[#] Michael G. B. Drew,[⊥] Golam Mostafa,*[,†] and Nirmalendu Ray Chaudhuri*[,‡]

Department of Physics, Jadavpur University, Kolkata 700032, India, Department of Inorganic Chemistry, Indian Association for the Cultivation of Science, Kolkata-700032, India, Department of Chemistry, School of Engineering and Physical Sciences, Heriot-Watt University, Riccarton, Edinburgh EH14 4AS, U.K., and Department of Chemistry, The University of Reading, Whiteknights, Reading RG6 6AD, U.K.

Received October 27, 2006; Revised Manuscript Received February 9, 2007

Ⓦ **This paper contains enhanced objects available on the Internet at http://pubs.acs.org/crystal.**

ABSTRACT: Three supramolecular complexes of Co(II) using $SCN^-/SeCN^-$ in combination with 4,4′-dipyridyl-*N*,*N*′-dioxide (dpyo), i.e., $\{[Co(SCN)_2(dpyo)_2]\cdot(dpyo)\}_n$ (**1**), $\{[Co(SCN)_2(dpyo)(H_2O)_2]\cdot(H_2O)\}_n$ (**2**), $\{[Co(SeCN)_2(dpyo)(H_2O)_2]\cdot(H_2O)\}_n$ (**3**), have been synthesized and characterized by single-crystal X-ray analysis. Complex **1** is a rare example of a dpyo bridged two-dimensional (2D) coordination polymer, and π-stacked dpyo supramolecular rods are generated by the lattice dpyo, passing through the rhombic grid of stacked layers, resulting in a three-dimensional (3D) superstructure. Complexes **2** and **3** are isomorphous one-dimensional (1D) coordination polymers [-Co-dpyo-Co-] that undergo self-assembly leading to a bilayer architecture derived through an $R_2^2(8)$ H-bonding synthon between coordinated water and dpyo oxygen. A reinvestigation of coordination polymers $[Mn(SCN)_2(dpyo)(H_2O)(MeOH)]_n$ (**4**) and $\{[Fe(SCN)_2(dpyo)(H_2O)_2]\cdot(H_2O)\}_n$ (**5**) reported recently by our group [Manna et al. *Indian J. Chem.* **2006**, *45A*, 1813] reveals brick wall topology rather than bilayer architecture is due to the decisive role of S···S/Se···Se interactions in determining the helical nature in **4** and **5** as compared to zigzag polymeric chains in **2** and **3**, although the same $R_2^2(8)$ synthon is responsible for supramolecular assembly in these complexes.

Introduction

Advancement in the field of supramolecular chemistry[2] and crystal engineering[3] during few last decades is noteworthy with a multitude of applications in various fields of chemistry such as molecular recognition,[4] sensors,[5] catalysis,[6] host−guest chemistry,[7] surface patterning,[8] electrical conductivity,[9] molecular sieves,[10] nonlinear optics,[11] etc. However, the full potential of this branch of chemistry is yet to be realized. The principle of designed synthesis of functional materials to some extent has been rationalized, but a multitude of factors especially the weak forces often come into play, and accurate prediction of the outcome of the crystallization process is yet to be realized. In this respect, it is very important to explore the role of weak interactions in crystal packing when a number of them are operating simultaneously. In recent times, 4,4′-dipyridyl-*N*,*N*′-dioxide (dpyo) has been increasingly used in crystal engineering as a potential ligand having the following advantageous features: (i) it is a long spacer that allows for construction of microporous materials with large cavities or channels; (ii) it possesses flexible coordination modes (*cis*-μ-4,4′; *trans*-μ-4,4′; μ-4,4; μ-4,4,4′,4′ and μ-4,4,4′) that may lead to novel topological architectures; (iii) it has a strong capability of forming hydrogen bonding and $\pi-\pi$ interaction—potential crystal engineering tools for tuning the supramolecular architecture; and (iv) its higher melting point allows the generation of materials with high thermal stability.[12] Only a limited number of compounds using this ligand have been documented until now,[13] and there is ample scope of further exploration in the field of crystal engineering and supramolecular chemistry using this ligand. Ambidentate short linear ligands SCN^- and $SeCN^-$ have been used by many research groups together with other rigid long spacers to design frameworks with different topologies. These pseudohalides when acting as bridging ligands sometimes provide a super exchange pathway[14] for magnetic interaction between successive metal centers, but more often it has been observed that they act as monodentate ligands to satisfy the coordination geometry of the metal ion.[15] In such complexes, pendant $SCN^-/SeCN^-$ often participate in weak hydrogen bonding,[16] but sometimes they also interact through S···S[17]/Se···Se[18] interactions, which influence the overall topology of the framework. It is noteworthy that dpyo bridged coordination polymers in combination with $SCN^-/SeCN^-$ are scarce, and only two complexes, $[Mn(SCN)_2(dpyo)(H_2O)(MeOH)]$ (**4**) and $[Fe(SCN)_2(dpyo)(H_2O)_2]\cdot(H_2O)$ (**5**), have been reported by our group recently.[1] In continuation, we have prepared a Co(II) analogue adopting the same reaction conditions, which is $\{[Co(SCN)_2(dpyo)_2]\cdot(dpyo)\}_n$ (**1**), displaying a two-dimensional (2D) rhombic grid structure with a π-stacked dpyo supramolecular rod inside the channel of the stacked grids, forming a three-dimensional (3D) supramolecular architecture. In an attempt to arrange the lattice dpyo molecules in the form of a molecular wire, a one-dimensional (1D) coordination polymer $[-Ag(I)-dpyo-Ag(I)-]_n$ passing through the rhomboidal grids, the previous reaction was carried out in the

* To whom correspondence should be addressed. (G.M.) E-mail: mostafa_ju@yahoo.co.in. (N.R.C.) E-mail: icnrc@iacs.res.in. Fax: (91) (33) 2473-2805.
[†] Jadavpur University.
[‡] Indian Association for the Cultivation of Science.
[#] Heriot-Watt University.
[⊥] The University of Reading.

10.1021/cg060762r CCC: $37.00
Published on Web 07/03/2007

Table 1. Crystallographic Data and Details of Refinements of Complexes 1−3

complex	1	2	3
empirical formula	$C_{32}H_{24}CoN_8O_6S_2$	$C_{12}H_{14}CoN_4O_5S_2$	$C_{12}H_{14}CoN_4O_5Se_2$
F_w	739.64	417.34	511.12
crystal system	monoclinic	triclinic	triclinic
space group	$P2_1/n$	$P\bar{1}$	$P\bar{1}$
a, Å	6.3084(3)	7.2846(9)	7.3668(8)
b, Å	13.7082(6)	9.820(2)	9.8897(11)
c, Å	18.1822(8)	12.0205(16)	12.0087(13)
α, °	90	77.731(15)	78.997(9)
β, °	99.075(2)	80.242(10)	80.858(9)
γ, °	90	88.515(14)	87.796(9)
volume, Å^3	1552.66(12)	828.0(2)	847.88(16)
Z	2	2	2
D_{calcd}, g cm^{-3}	1.582	1.674	2.002
μMoKα, (mm^{-1})	0.748	1.319	5.335
F(000)	758	426	498
reflections collected	63629	5730	6040
unique reflections	7218	4571	4767
R_{int}	0.025	0.037	0.028
θ_{max} (°)	36.4	30.2	30.1
observed $I > 2\sigma(I)$	5958	3095	2783
parameters	223	235	235
goodness of fit (F^2)	1.10	1.08	0.88
$R1$ ($I > 2\sigma(I)$) [a]	0.0319	0.0809	0.0428
$wR2$ [a]	0.0902	0.2630	0.1006
$\Delta\rho$ (e/Å^3)	−0.36, 1.10	−0.77, 2.59	−0.91, 1.97

[a] $R1 = \sum||F_o| - |F_c||/\sum|F_o|$, $wR2 = [\sum w(F_o^2 - F_c^2)^2/\sum w(F_o^2)^2]^{1/2}$.

presence of Ag(I) salt. In contrast to our expectation, the product obtained was again a dpyo bridged 1D coordination polymer, $\{[Co(SCN)_2(dpyo)(H_2O)_2]\cdot(H_2O)\}_n$ (**2**). The reaction of Co(II) with dpyo in the presence of $SeCN^-$ also resulted a 1D coordination polymer, $\{[Co(SeCN)_2(dpyo)(H_2O)_2]\cdot(H_2O)\}_n$ (**3**). Complexes **2** and **3** are isomorphous, and supramolecular assembly into a bilayer architecture is due to the tendency of these chains to self-assemble through the formation of an $R_2^2(8)$ hydrogen-bonded synthon between dpyo oxygen and coordinated water of two adjacent chains. An attempt to compare the supramolecular assembly of the complexes (**2**, **3**) with (**4**, **5**) reveals brick wall (in the *bc* plane) and rectangular grid (in the *ac* plane) topology in the overall 3D supramolecular assembly of these complexes instead of bilayer architecture observed in **2** and **3**, although the same $R_2^2(8)$ synthon is responsible for their self-assembly. A deeper investigation behind this architectural variation in self-assembly of 1D polymeric chains of (**2**, **3**) and (**4**, **5**) has led us to unravel that S···S/Se···Se interaction is responsible for this. Besides describing the rare 2D coordination polymer (complex **1**), we report also the importance of relatively weaker forces, i.e., S···S/Se···Se interactions, in determining the ultimate supramolecular assembly in the solid state.

Experimental Section

Materials. High purity 4,4′-dipyridyl-*N*,*N*′-dioxide (98%) was purchased from Aldrich Chemical Co. and was used as received. All other chemicals were of AR grade.

Physical Measurements. Elemental analyses (C, H, N) were performed using a Perkin-Elmer 240C elemental analyzer. IR spectra were measured from KBr pellets on a Nicolet 520 FTIR spectrometer. The magnetic susceptibility was measured at 27 °C using an EG and G PAR-155 vibrating sample magnetometer, using $Hg[Co(SCN)_4]$ as reference material; diamagnetic correction was made by using Pascal's constant. Thermal analyses were carried out on a Perkin-Elmer Pyris Diamond system.

Synthesis of $\{[Co(SCN)_2(dpyo)_2]\cdot(dpyo)\}_n$ (1). An aqueous solution (5 mL) of ammonium thiocyanate (0.152 g, 2 mmol) was added to an aqueous solution (5 mL) of $Co(NO_3)_2\cdot6H_2O$ (1 mmol; 0.291 g) with constant stirring. To the resulting deep pink-colored reaction mixture, a methanolic solution (10 mL) of dpyo (0.188 g, 1 mmol) was added and stirred for 30 min. A pink-colored complex was separated out. The pink crystals suitable for X-ray analysis were obtained by diffusing the methanolic solution (10 mL) of dpyo on an aqueous (10 mL) layer containing $Co(NO_3)_2\cdot6H_2O$ and ammonium thiocyanate (1:1) in a tube. The pink-colored crystals were deposited at the junction of two layers after a few days. Yield: 68%. Anal. Calcd for $C_{32}H_{24}CoN_8O_6S_2$ (739.64): C, 51.91; H, 3.24; N, 15.14 (%). Found: C, 50.32; H, 3.16; N, 14.82(%). The infrared spectra exhibited the following absorptions: 2075(vs), 1633(w), 1478(w), 1440(vw), 1205(w), 1183(w), 830(s), 678(s), 565(vw) cm^{-1}. Room-temperature magnetic moment: μ_{eff} = 5.04, μ_B at 300 °C.

Synthesis of $\{[Co(SCN)_2(dpyo)(H_2O)_2]\cdot(H_2O)\}_n$ (2). It was prepared using a diffusion technique. A methanolic solution (10 mL) of a mixture of dpyo (1.25 mmol, 0.235 g) and $AgNO_3$ (0.25 mmol, 0.042 g) was diffused on an aqueous layer (10 mL) of cobalt nitrate hexahydrate (0.50 mmol, 0.145 g) and ammonium thiocyanate (1 mmol, 0.076 g) mixture in a tube. Pink crystals suitable for X-ray analysis were obtained at the junction of the two solutions after a few days. Yield: 70%. Anal. Calcd for $C_{12}H_{14}CoN_4O_5S_2$ (417.34): C, 34.50; H, 3.35; N, 13.42(%). Found: C, 35.02; H, 3.42; N, 12.98(%). The infrared spectra exhibited the following absorptions: 3490−3000(sbr), 2100(vs), 2075(vs), 1660(w), 1624(w), 1480(s), 1427(s), 1324(vw), 1205(vs), 1186(vs), 829(s), 673(vs), 555(w), 522(vw), 476(vw) cm^{-1}. Room-temperature magnetic moment (μ_{eff}) = 5.03 μ_B at 300 °C.

Synthesis of $\{[Co(SeCN)_2(dpyo)(H_2O)_2]\cdot(H_2O)\}_n$ (3). It was synthesized following the procedure adopted for complex **1** using potassium selenocyanate instead of ammonium thiocyanate (0.287 g, 2 mmol). The single crystals suitable for X-ray analysis were obtained by diffusing the methanolic solution (10 mL) of dpyo on an aqueous (10 mL) layer containing $Co(NO_3)_2\cdot6H_2O$ and potassium selenocyanate (1:1) in a tube. The deep pink-colored crystals were deposited at the junction of two layers after a few days. Yield: 72%. Anal. Calcd for $C_{12}H_{14}CoN_4O_5Se_2$ (511.12): C, 28.17; H, 2.73; N, 10.95(%). Found: C, 27.49; H, 2.61; N, 11.21(%). The infrared spectra exhibited the following absorptions: 3485−3030(sbr), 2090(vs), 1620(w), 1548(w), 1471(vs), 1425(s), 1325(vw), 1261(vs), 1217(vs), 180(vs), 1026(s), 964(w), 833(vs), 700(w), 557(s), 476(w), 428(vw) cm^{-1}. Room-temperature magnetic moment (μ_{eff}) = 5.00 μ_B at 300 °C.

Crystallographic Data collection, Structure Solution, and Refinement. Crystal data and details of data collections and refinements for the complexes are reported in Table 1. Intensity data were collected using MoKα (λ = 0.71073 Å) radiation by mounting the crystals of **1** on a Bruker AXS P4 diffractometer equipped with a graphite monochromator, and for complexes **2** and **3** a modified STOE four-circle diffractometer equipped with a Mar-research Image Plate was used.

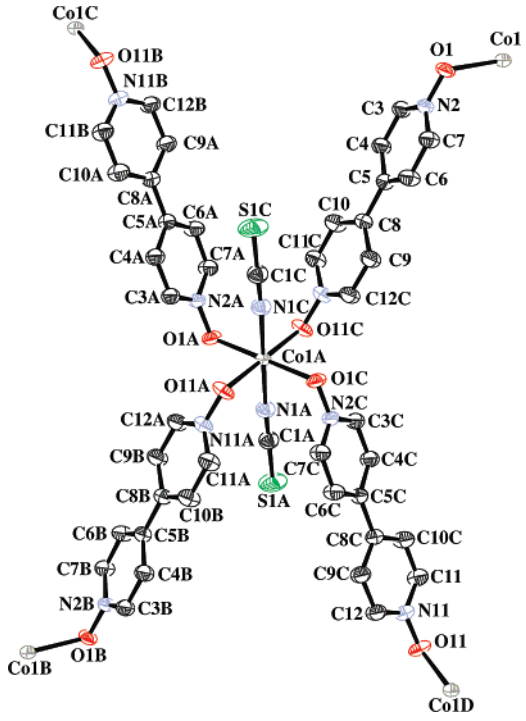

Figure 1. ORTEP diagram (50% ellipsoidal probability) of a part of the 2D coordination polymer of complex **1** with atom labeling scheme.

Table 2. Selected Bond Lengths (Å) and Angles (°) for Complex 1

Co1−O1	2.1095(7)	N1−C1	1.1703(12)
Co1−O11	2.0533(7)	S1−C1	1.6418(9)
Co1−N1	2.0967(7)		
O1−Co1−O11	89.17(3)	Co1−O1−N2	116.12(5)
O1−Co1−N1	87.97(2)	Co1−O11−N11	121.13(5)
O11−Co1−N1	91.41(3)	Co1−N1−C1	170.04(8)
S1−C1−N1	178.89(9)		

Cell refinement, indexing, and scaling for the data sets were performed by using XDS,[19] Denzo,[20] Scalepack,[20] and Crystal package[21] programs. All the structures were solved by Patterson methods and subsequent Difference Fourier synthesis.[22] Structures were refined by the full-matrix least-squares method based on F^2.[22] Hydrogen atoms positions were determined using riding atom model. All the calculations were performed using the WinGX System, Ver 1.70.00,[23a] PLATON 2003,[23b] and ORTEP-32.[24]

Results and Discussion

Structure Description of Complex 1. The coordination environment around Co(II) centers has near perfect octahedral geometry (Figure 1) as the Co(II) atom occupies the center of symmetry. Co−O and Co−N distances vary within the range 2.05−2.10 Å, which are comparable to that observed in similar complexes.[25] The bond distances and angles are given in Table 2. Four dpyo ligands bind the Co(II) center in trans mode using one of the lone pairs available at the oxygen atom and form the equatorial plane of the Co(II) center. The N atoms of two pendant SCN ligands occupy trans axial positions of the octahedron. The octahedron is slightly elongated along the axial direction, which is reflected in the slightly larger Co−N distances.

X-ray crystal structure reveals that the complex consists of 2D polymeric sheets with rhombic channels (Figure 2). This is a rare[25e] dpyo bridged 2D polymer, where using its trans binding mode dpyo ligands have joined Co(II) centers into a 2D polymeric sheet. The polymeric sheets are the (101) planes of the crystal. The rhombic grids have the dimension 12.19 × 12.19 Å. Two angles of the rhombus are 68.42° and 111.58°, respectively. The long diagonal of the rhombus is 20.164 Å, and the short diagonal is 13.708 Å.

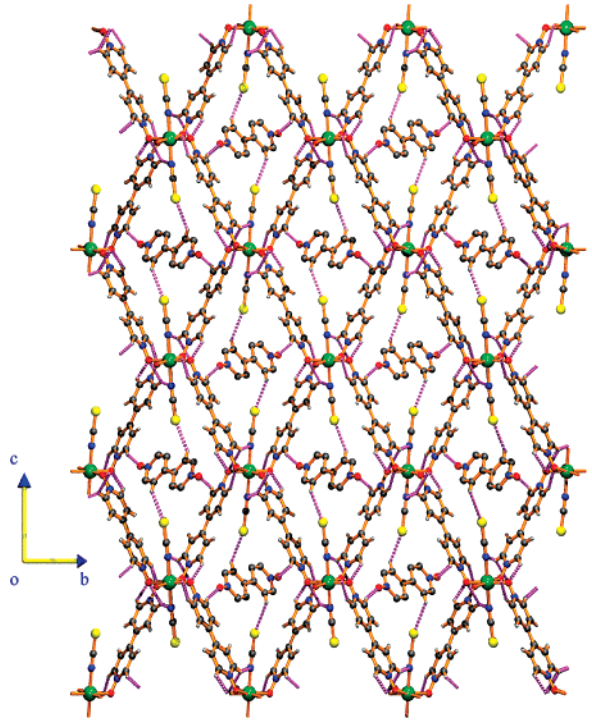

Figure 2. Rhombic grids of complex **1** incorporating lattice dpyo molecules through hydrogen bonding.

Ⓦ A 3D rotatable image in XYZ format is available.

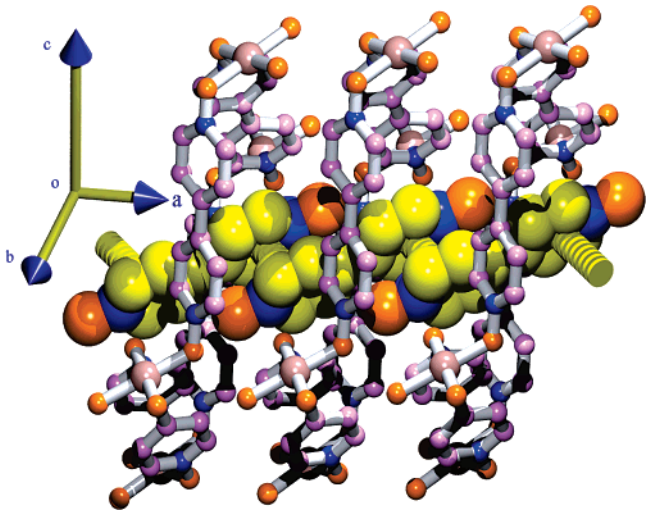

Figure 3. π-Stacked dpyo molecular rod passes through the channel in **1** and reinforces stacking of successive 2D layers into 3D. $\pi\cdots\pi$ interactions between rod and grid dpyo molecules have not been shown for clarity.

Ⓦ A 3D rotatable image in XYZ format is available.

The stacking of these polymeric sheets along the crystallographic *a*-axis has been achieved in a very interesting way. Lattice dpyo molecules arrange themselves in the form of a supramolecular rod by interacting with each other by $\pi\cdots\pi$ interaction (Figure 3, Table S1, Supporting Information) and pass through the channels. The $\pi\cdots\pi$ interaction between the free dpyo ligands forming the molecular rod is quite strong with a ring centroid distance of 3.55 Å and 0° dihedral angle between

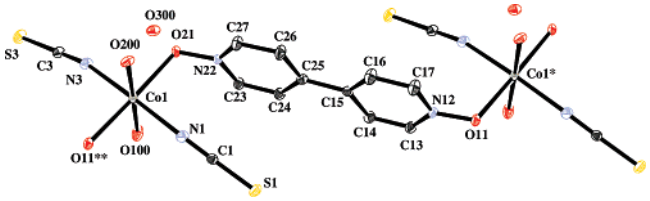

Figure 4. ORTEP diagram (50% ellipsoidal probability) of complex **2** with atom labeling scheme.

Table 3. Selected Bond Lengths (Å) and Angles (°) for Complexes 2 and 3

	Complex **2**		
Co1−O11	2.115(5)	Co1−O100	2.101(5)
Co1−O21	2.111(5)	Co1−O200	2.142(5)
Co1−N1	2.067(6)	Co1−N3	2.056(6)
O11−Co1−O21	176.5(2)	Co1−O11−N12	115.8(3)
O100−Co1−O200	178.5(2)	Co1−O21−N22	115.9(3)
N1−Co1−N3	174.4(2)	Co1−N1−C1	163.7(6)
S1−C1−N1	178.2(6)	Co1−N3−C3	165.7(6)
S3−C3−N3	178.1(7)		
	Complex **3**		
Co3−O1	2.117(3)	Co3−O101	2.153(3)
Co3−O72	2.112(3)	Co3−N41	2.050(4)
Co3−O100	2.091(3)	Co3−N51	2.058(4)
O1−Co3−O72	176.86(12)	O100−Co3−N51	87.31(15)
O100−Co3−O101	178.76(13)	O101−Co3−N41	93.20(13)
O100−Co3−N41	87.35(13)	O101−Co3−N51	92.15(14)
Co3−O1−N2	114.7(2)	Co3−N41−C42	164.3(3)
Co3−O72−N71	115.3(2)	Co3−N51−C52	164.1(4)
Se43−C42−N41	177.0(4)	Se53−C52−N51	177.3(4)

the ring normal of successive dpyo rings. The support to the main framework by this molecular rod is through the $\pi\cdots\pi$ interaction of this rod with the dpyo rings forming the grid wall (Table S1, Supporting Information, Figure 3). A single unit of the rod (a single dpyo molecule positions itself within two grids) piercing through the channel interacts with the grid wall of two adjacent polymeric sheets. C−H···O weak hydrogen bonding (Table S2, Supporting Information) between the grid wall pyridine CH group and two terminal O atoms of the channel dpyo ligands reinforces the contact between adjacent layers. Another C−H···S (C25−H25···S1) contact between the CH group of channel dpyo and S atoms of the pendant SCN^- ligands also assists in this packing.[16] The interplanar spacing of 6.308 Å between adjacent polymeric sheets is the result of cooperative interaction of all these weak interactions working in unison. The $\pi\cdots\pi$ interaction results in the rhombic shape of individual grids and induces strain in the grid dpyo molecules, which has a dihedral angle of 8.62(9)° between its pyridine ring planes. The free dpyo ligands are strain-free with the dihedral angle between the ring planes being 0°. The stacking of the polymeric grids is thus achieved through the $\pi\cdots\pi$ interaction with the molecular rods passing through its channels, and supramolecular assembly in this mode is novel to the best of our knowledge.

Structure Description of Complexes 2 and 3. X-ray structural analysis of complex **2** reveals 1D polymers comprising of two dpyo, two thiocyanate anions, and two water molecules around the Co(II) coordination sphere (Figure 4). Two trans N atoms of two thiocyanates and two trans oxygen atoms of two dpyo form the equatorial plane of the octahedron. Two water molecules occupy trans axial positions. The Co(II) coordination sphere is a slightly distorted octahedron. The coordination bond (Co−O) distances for the dpyo ligands are comparable with those described in the literature (Table 3).[25] The Co−O−N bond angles are 115.8(3)° (for Co1−O11−N12) and 115.9(3)° (for Co1−O21−N22). The polymeric chain thus formed is a zigzag one, but all the Co(II) centers align in a line. The line joining

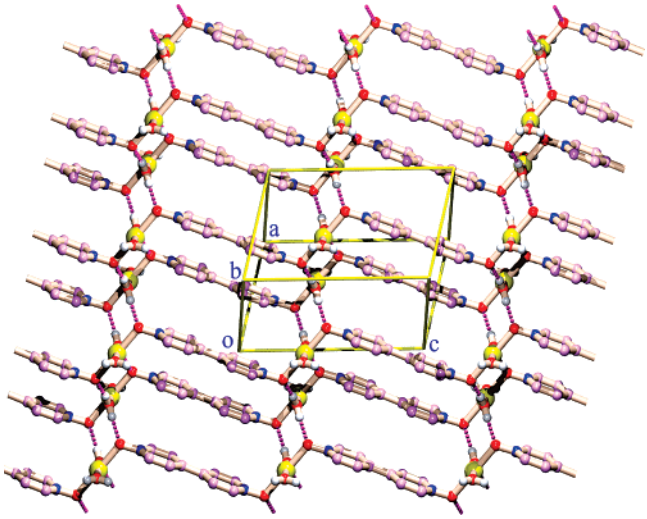

Figure 5. Hydrogen-bonded bilayer architecture of the complex in the *ac* plane (pseudo halides have been omitted for clarity).

Ⓦ A 3D rotatable image in XYZ format is available.

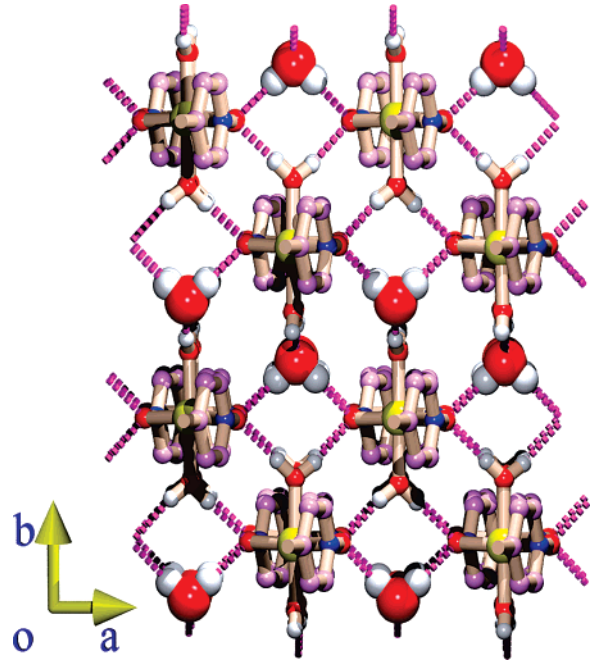

Figure 6. Interlayer water molecules linking supramolecular bilayers along the crystallographic *b*-axis leading to a 3D super assembly in the complex (pseudohalides have been omitted for clarity).

Ⓦ A 3D rotatable image in XYZ format is available.

the metal centers bisects dpyo molecules symmetrically. Thus, the polymeric chains are aligned along the crystallographic *c*-axis. Two sets of these chains self-assemble into a 2D sheet in the *ac* plane. The sheet is doubly layered (Figure 5). In this novel assembly of Co(II) with dpyo ligands, trans axial water molecules forming the inner side of the bilayer interlock two adjacent polymeric chains through $R_2^2(8)$ hydrogen bonding (Table S3, Supporting Information) with the dpyo oxygen. To facilitate this hydrogen bonding, one set of chains positions them slightly above the equatorial plane of the other set. Stacking of the 2D layers along the crystallographic *b*-axis is shown in Figure 6. This stacking is facilitated by lattice water molecules, which by hydrogen bonding with coordinated water act as a "Y"-type connector between successive layers. Within each layer

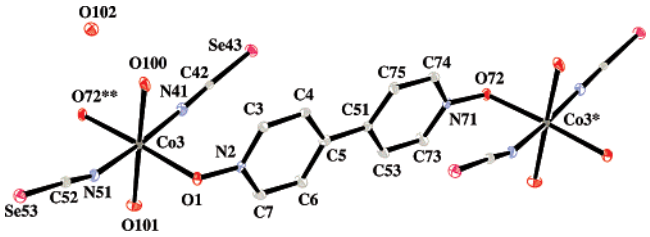

Figure 7. ORTEP diagram (50% ellipsoidal probability) of complex **3** with atom labeling scheme.

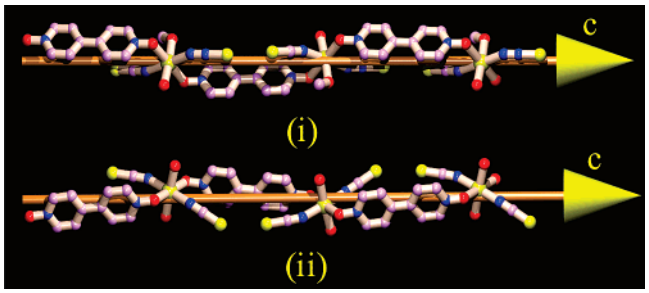

Figure 8. Helical 1D coordination polymers for complex **4** (i) and complex **5** (ii) running along the crystallographic *c*-axis.

adjacent chains interact via interchain S···S interaction (distance 3.655(3) Å, which is lower than the sum of the van der Waals radii (4.06 Å) of S atoms[26]) and S···π interaction (Table S4, Supporting Information, Figure 12). The intra dpyo ring plane twist in the complex is 0.8(3)°.

Complex **3** is isomorphous to complex **2**. $SeCN^-$ in **3** plays an analogous role of SCN^- in **2** and binds the Co(II) center (Figure 7) through an N atom. The Co−O bond distances in this case range from 2.091(3) to 2.117(3) Å (Table **3**). Co−O···N bond angles are 114.7(2) and 115.3(2)°. The interchain Se−Se distance in this case is 3.4960(8) Å and is very much less than the sum of the van der Waals radii (4.30 Å) of Se atoms,[26] indicating strong Se···Se interaction. There is also an interchain Se···π interaction (Table S5, Supporting Information). The intra dpyo ring plane twist angle is 5.6(2)°. The crystal packing is similar to complex **2** leading to bilayers stitched by lattice water molecules.

Structural Aspects and Supramolecular Assembly in Complexes 4 and 5. The X-ray structures were reported by us.[1] The additional structural features not reported earlier is the helical nature of the polymeric chains (Figure 8). The pitch values of the helices are 24.27(3) and 24.0226(10) Å, respectively. The successive coordination sphere is rotated by 180° along helical chains, and the chains are aligned along the crystallographic *c*-axis. Side by side alignment of these chains are determined by the $R_2^2(8)$ hydrogen-bonding synthon,[27] generated through the coordinated water molecule of one chain and O atoms of dpyo molecules of the adjacent chain. Two sets of this $R_2^2(8)$ hydrogen-bonding synthons are operative, one along the *a*-axis and the other along the *b*-axis, which is responsible for respective supramolecular sheets in the *ac* and *bc* planes. The interesting feature in the packing is that when one considers the *ac* plane, adjacent helical chains are all identical (Figure 9) but in the *bc* plane adjacent helical chains are racemic (Figure 10) to each other. As a result, the topologies of these sheets are quite different: one has rectangular hydrogen-bonded networks, but the other has a brick wall topology with sausage-shaped bricks. The brick wall topology has arisen exclusively due to (i) the helical nature of the polymeric chains and (ii) side by side alignment of oppositely running helices,

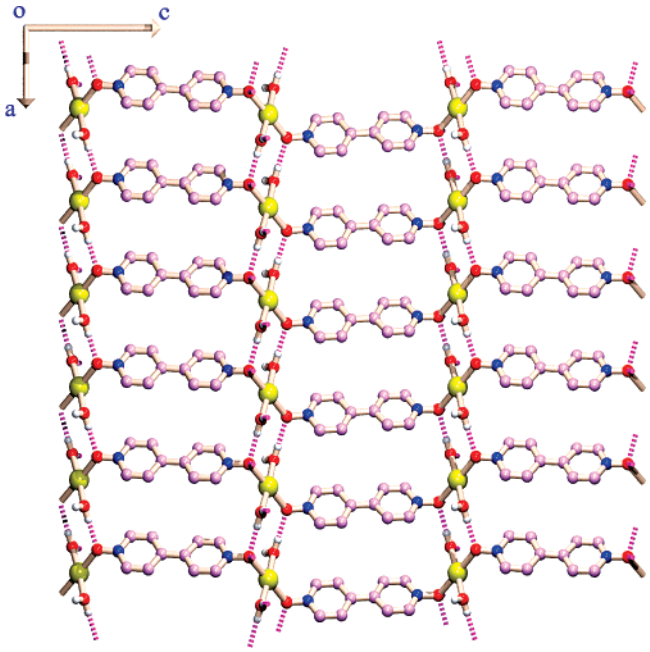

Figure 9. $R_2^2(8)$ synthon involving coordinated water and dpyo O atom assembles the 2D sheet (*ac* plane) of helices with the same chirality in complex **4** (pseudohalides have been omitted for clarity). Complex **5** has a similar architecture with one of the coordinated water's role played by coordinated methanol.

Ⓦ A 3D rotatable image in XYZ format is available.

which form successive supramolecular contacts at their nearest points, which are a half screw pitch away from each other. A deeper search for the reason behind the helical nature of the chains in **4** and **5** reveals that it is the result of relatively weaker forces, namely, S···S and S···π[28] interactions (Table S4, Supporting Information). These forces are responsible for the helical nature of these coordination polymers. The intrachain S···S distance in complex **4** is 3.541(3) Å, and in **5** it is 3.605(1) Å, which are well within the sum of van der Waals radii of S atoms, which is 4.06 Å.[26] Although these interactions are assumed to be relatively weaker, here they have become competitive enough to influence the overall chain topology. In its presence, successive metal coordination environments along a chain are tilted inward and outward alternately and result in the helical nature of the chain. The M−O−N angles at successive metal centers are 119.1(3)° and 124.0(3)° for complex **4**, whereas they are 118.5 (1)° and 122.9(1)° for complex **5**. There are approximately 4.9° and 4.4° differences in successive M−O−N bond angles in complexes **4** and **5**, respectively. There is also an intra-dpyo ring plane twist of 3.1(3)° and 6.8(1)° in complexes **4** and **5**, respectively. This can be attributed to the cooperative operation of S···S and S···π interactions, resulting into the helical nature of the chain.

Thermal Analysis. Complex **1** is thermally stable up to 300 °C, and on further heating it collapses. Thermogravimetric analysis of complex **2** reveals that it is stable up to 50 °C, and on further heating it loses one lattice and two coordinated water molecules in single step (weight loss, observed: 13.22, calculated: 12.94%) yielding as blue species **2a**, which is stable up to 250 °C, but collapses beyond this temperature. Complex **3** upon heating shows no mass change up to 75 °C, and on further heating it loses water molecules in two steps. The first step (75−110 °C) corresponds to the loss of one lattice water molecule (weight loss, observed: 4.12, calculated: 3.52%) yielding the intermediate species $[Co(SeCN)_2(dpyo)(H_2O)_2]$ (**3a**). The species

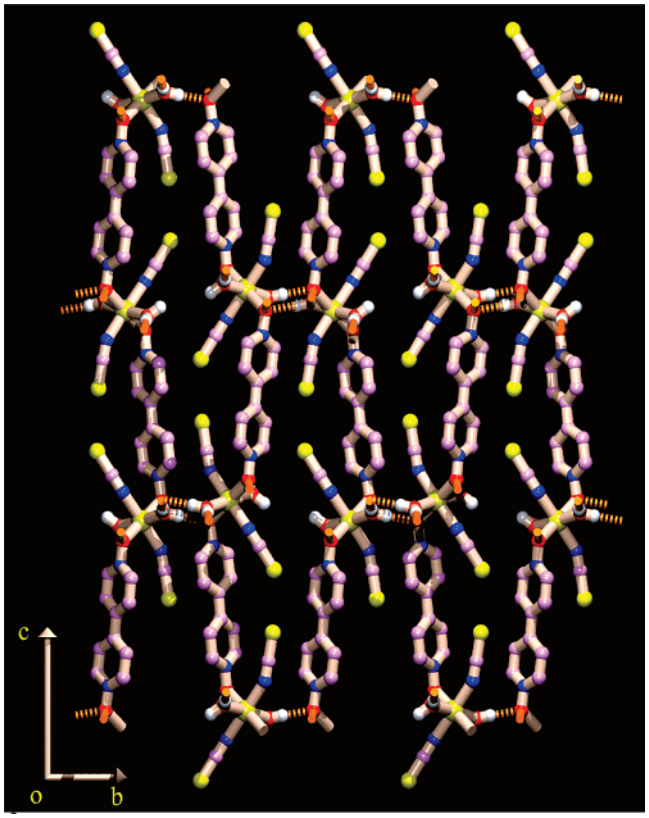

Figure 10. $R_2^2(8)$ synthon involving coordinated water and dpyo O atom assembles the 2D sheet (*bc* plane) of alternate racimate helices in complex **5.** Complex **4** has exactly identical architecture with ligated methanol replaced by coordinated water.

Ⓦ A 3D rotatable image in XYZ format is available.

3a is stable up to 245 °C and on further heating starts to lose two coordinated water molecules and becomes deaquated (weight loss, observed: 7.35, calculated: 7.04%) at 280 °C. The species collapses immediately as soon as dehydration is completed.

Comparative Structural Features of Complexes 2−5. Overall 3D supramolecular assembly of the polymeric chains in complexes **2**−**5** is primarily determined by hydrogen bonding interactions between adjacent chains through the formation of a $R_2^2(8)$ H-bonding synthon between coordinated water and dpyo oxygen atoms. A literature survey[12,25a,d] reveals that this synthon is also responsible for the supramolecular assembly of similar 1D polymeric chains involving dpyo ligands.

In complexes **2** and **3**, $R_2^2(8)$ H-bonding synthon mediated assembly of chains lead to the formation of bilayer topology. The monolayers of the bilayer are interlocked with each other at the midpoint through hydrogen bonding between coordination water and dpyo O atoms. On either side of the bilayer, remaining coordinated waters form hydrogen bonds with lattice water molecules. These lattice water molecules function as "Y"-shaped connectors between adjacent bilayers and stack them along the crystallographic *b* direction.

In complexes **4** and **5** a similar $R_2^2(8)$ H-bonding synthon propagates the assembly in two perpendicular directions, which are perpendicular to the chain direction. As a result 2D H-bonded sheets both in the *ac* and *bc* planes could be visualized. The interesting point to be noted is that the architecture in the *ac* plane is a rectangular grid, whereas that in the *bc* plane it has a brick wall topology. Brick wall topology is the result of the helical nature of the polymeric chains, in

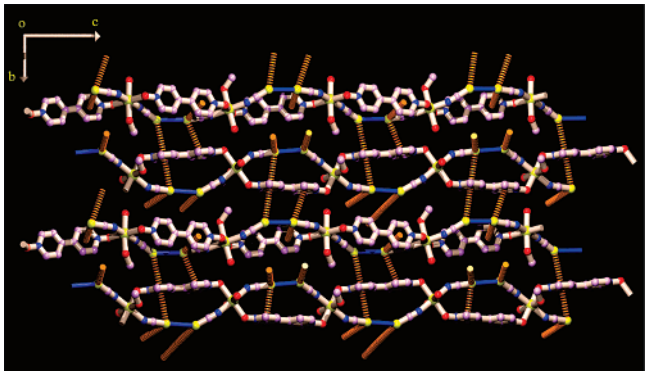

Figure 11. Structure-directing role of intrachain S···S and interchain S···π interactions in complexes **4** and **5**.

Ⓦ A 3D rotatable image in XYZ format is available.

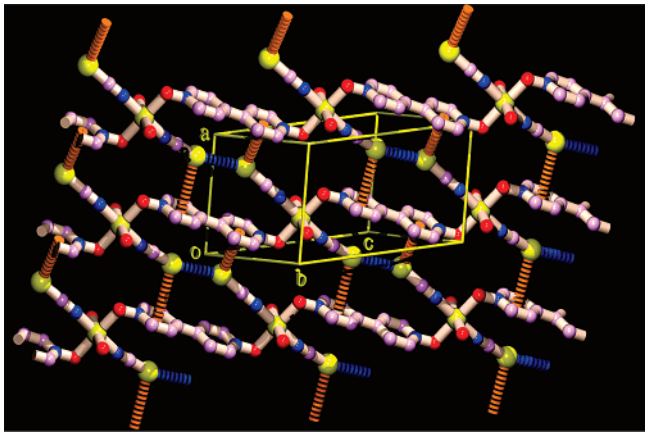

Figure 12. Interchain S···S/Se···Se and S···π/Se···π interactions operating within a monolayer of the bilayer sheet for complexes **2** and **3**.

Ⓦ A 3D rotatable image in XYZ format is available.

which adjacent helices are racemic and establish hydrogen-bonding contacts wherever they come closer to each other. Rectangular grid topology in the *ac* plane is due to the assembly of helices with similar handedness. To the best of our knowledge, helical coordination polymers of dpyo ligands have not been observed earlier together with its consequent brick wall topology.

A closer look into the structures reveals that the architectural variation into brick wall and bilayer topology is the result of the influence of comparatively weaker forces in the hierarchy, namely, the S···S/Se···Se and S···π/Se···π interactions. In complexes **4** and **5**, S···S interaction is intrachain (Figure 12), whereas S···S and Se···Se interactions are interchain in complexes **2** and **3** (Figure 11), respectively. Intrachain S···S contacts in **4** and **5** tilt adjacent coordination spheres by slightly perturbing them and must be responsible for the formation of coordination helix. In complexes **2** and **3**, as this force is interchain and directs away from the chain axis, adjacent metal coordination environments are identical, having a center of symmetry at the middle of the bridging dpyo molecule resulting a zigzag chain instead of a helix. The resultant architectural variation of the supramolecular assembly is the outcome of this basic difference of the dpyo bridged polymeric chains. Relatively less known S···π and Se···π interactions are well established for their relevance in biological processes such as protein folding.[28a,b] Favorable distances for these interactions in complexes **2**−**5** hint that in inorganic environments they also can

be influential. In complexes **4** and **5**, a linear and angular sandwiched S···π pattern is observed (Figure 11), but in complexes **2** and **3** a symmetric S···π pattern is observed (Figure 12).

To investigate the abundances of SCN^- and $SeCN^-$ complexes in which SCN^- or $SeCN^-$ take part in S···S/Se···Se or S···π/Se···π interactions, a Cambridge Structural Database (CSD) search was carried out with the help of ConQuest program (version 1.8) on the November 2005 release of the CSD version 5.27. A search on organometallic compounds having an R-factor less than 10% and a query for S···S nonbonded interaction between two SCN^- fragments with S···S distance constrained to be less than 4.0 Å (slightly smaller than the sum of the van der Waals radii, which is 4.06 Å for S and 4.30 Å for Se)[26] resulted in 809 hits. A similar search for Se···Se interactions resulted in 23 hits. A search for S···π and Se···π interactions involving SCN^- and $SeCN^-$ with a pyridine ring having no side group with a distance constraint of less than 4 Å between SCN^-/$SeCN^-$ and a pyridine ring centroid resulted in 249 and 17 hits, respectively. Similar searches for SCN^- and $SeCN^-$ with a phenyl ring having no side group resulted in 385 and 13 hits, respectively. These results indicate that S···S/Se···Se and S···π /Se···π interactions involving SCN^- and $SeCN^-$ is abundant for metal−organic complexes. A relatively fewer number of hits for Se···Se and Se···π interactions is most probably due to fewer numbers of $SeCN^-$ bearing complexes in the CSD. The above search results indicate the existence of these interactions in metal−organic complexes. A correct analysis of the true nature of these interactions needs careful study of the interaction geometries in each individual complex together with quantum chemical calculations on systems involving SCN^- and $SeCN^-$. Theoretical investigations of these interactions have been carried out recently[28c] for model systems, but further work is needed for complete understanding. A combined database and theoretical study on these systems is currently in progress and will be reported in the future.

Conclusion

In summary, three Co(II) and one each of Fe(II) and Mn(II) complexes with dpyo and SCN^-/$SeCN^-$ have been synthesized and characterized by X-ray crystallography. To the best of our knowledge, complex **1** is the second example of a 2D grid network of dpyo molecules. The novelty in the supramolecular assembly of the complex is the support by the π-stacked molecular rods for 3D stacking of the polymeric sheets passing through channels.

Structural variation in complexes **2**−**5** has been analyzed, which reveals that although the same $R_2^2(8)$ hydrogen-bonding synthon drives the assembly of these chains the helical nature gives rise to brick wall topology, and the centrosymmetric zigzag nature of the chains is responsible for the bilayer architecture. In the assembly of these complexes, a coordinative force plays the role of forming 1D chains and comparatively weaker O−H···O hydrogen bonding forces assemble these chains into sheets. Weakest S···S/Se···Se and S···π/Se···π forces also subtly influence the overall assembly by tuning the chains into helices in complexes **2** and **3** and by nullifying each other in complexes **4** and **5**, operating symmetrically in opposite directions leading to a zigzag nature of the chains in these complexes. To conclude, weakest of interactions such as S···S and S···π should be carefully analyzed. Surprising roles played by such forces could be uncovered. CSD analysis also corroborates this.

Supporting Information Available: X-ray crystallographic data, in CIF format, and other crystallographic information are available free of charge via the Internet at http://pubs.acs.org.

References

(1) Manna, S. C.; Zangrando, E.; Okamoto, K.; Ray Chaudhuri, N. *Indian J. Chem.* **2006**, *45A*, 1813.

(2) (a) *Comprehensive Supramolecular Chemistry*; Atwood, J. L.; Davies, J. E. D.; Mac Nicol, D. D.; Vogtle, F.; Lehn, J. M., Eds. Pergamon: Oxford, UK, 1996; Vol. 6. (b) *Crystal Engineering*: *The Design and Applications of Functional Solids*; Seddon, K. R., Zaworotko, M. J., Eds.; NATO ASI Series; Kluwer Academic: Dordrecht, The Netherlands, 1998. (c) *Crystal Engineering*: From Molecules and Crystals of Materials; Braga, D., Grepioni, F., Orpen, A. G., Eds.; NATO ASI Series; Kluwer Academic: Dordrecht, The Netherlands, 1999. (d) *Design of Organic Solids; Topics in Current Chemistry Series*; Weber, E., Ed.; Springer-Verlag: Berlin, Heidelberg, Germany, 1998; Vol. 198. (e) *Molecular Self-Assembly Organic Versus Inorganic Approaches; Structure and Bonding Series*; Fujita, M., Ed.; Springer-Verlag: Berlin, Heidelberg, Germany, 2000; Vol. 96. (f) Kubo, Y.; Kitada, Y.; Wakabayashi, R.; Kishida, T.; Ayabe, M.; Kaneko, K.; Takeuchi, M.; Shinkai, S. *Angew. Chem., Int. Ed.* **2006**, *45*, 1548. (g) Tiedemann, B. E. F.; Raymond, K. N. *Angew. Chem., Int. Ed.* **2006**, *45*, 83. (h) Tsuda, A.; Hu, H.; Tanaka, R.; Aida, T. *Angew. Chem., Int. Ed*. **2005**, *44*, 4884. (i) Eckel, R.; Ros, R.; Decker, B.; Mattay, J.; Anselmetti, D. *Angew. Chem., Int. Ed*. **2005**, *44*, 484.

(3) (a) Moulton, B.; Zaworotko, M. J. *Chem. Rev.* **2001**, *101*, 1629. (b) Kim, K. *Chem. Soc. Rev*. **2002**, *31*, 96. (c) Evans, R. O.; Lin, W. *Acc. Chem. Res*. **2002**, *35*, 511.

(4) (a) Kondo, M.; Yoshitomi, T.; Seki, K.; Matsuzaka, H.; Kitagawa, S. *Angew. Chem., Int. Ed. Engl.* **1997**, *36*, 1725. (b) Ghosh, A. K.; Jana, A. D.; Ghoshal, D.; Mostafa, G.; Ray Chaudhuri, N. *Cryst. Growth Des.* **2006**, *6*, 701.

(5) Sun, S.-S.; J. Lees, A. J. *Coord. Chem. Rev.* **2002**, *230*, 171.

(6) Maruoka, K.; Murase, N.; Yamamoto, H. *J. Org. Chem.* **1993**, *58*, 2938.

(7) (a) Maji, T. K.; Mukherjee, P. S.; Mostafa, G.; Zangrando, E.; Ray Chaudhuri, N. *Chem. Commun.* **2001**, 1368. (b) Yaghi, O. M.; Li, G.; Li, H. *Nature* **1995**, *378*, 703. (c) Hagrman, P. J.; Hagrman, D.; Zubieta, J. *Angew. Chem., Int. Ed.* **1999**, *38*, 2638. (d) Li, H.; Eddaoudi, M.; Okeeffe, M.; Yaghi, O. M. *Nature* **1999**, *402*, 276. (e) Kepert, C. J.; Rosseinsky, M. J. *Chem. Commun.* **1999**, 375. (f) Niu, T.; Jacobson, A. J. *Inorg. Chem.* **1999**, *38*, 5346. (g) Gudbjartson, H.; Biradha, K.; Poirer, K. M.; Zaworotko, M. J. *J. Am. Chem. Soc.* **1999**, *121*, 2599. (h) Goodgame, D. M. L.; Grachvogel, D. A.; Willams, D. J. *Angew. Chem., Int. Ed.* **1999**, *3*, 641. (i) MacGillivray, L. R.; Groenman, R. H.; Atwood, J. L. *J. Am. Chem. Soc.* **1998**, *120*, 2676.

(8) (a) Puigmarti-Luis, J.; Minoia, A.; Uji-i, H.; Rovira, C.; Cornil, J.; De Feyter, S.; Lazzaroni, R.; Amabilino, D. B. *J. Am. Chem. Soc.* **2006**, *128*, 12602. (b) Clair, S.; Pons, S.; Brune, H.; Kern, K.; Barth, J. V. *Angew. Chem., Int. Ed.* **2005**, *44*, 7294. (c) Kubo, Y.; Kitada, Y.; Wakabayashi, R.; Kishida, T.; Ayabe, M.; Kaneko, K.; Takeuchi, M.; Shinkai, S. *Angew. Chem., Int. Ed.* **2006**, *45*, 1548.

(9) Hoskins, B. F.; Robson, R. *J. Am. Chem. Soc*. **1990**, *112*, 1546.

(10) Yuan, A.; Zou, J.; Li, B.; Zha, Z.; Duan, C.; Liu, Y.; Xu, Z.; Keizer, S. *Chem. Commun.* **2000**, 1279.

(11) Chen, C.; Suslick, K. S. *Coord. Chem. Rev.* **1993**, *128*, 293.

(12) Ma, B.-Q.; Sun, H.-L.; Gao, S.; Xu, G.-X. *Inorg. Chem.* **2001**, *40*, 6247.

(13) (a) Long, D. L.; Blake, A. J.; Champness, N. R.; Wilson, C.; Schröder, M. *Angew. Chem., Int. Ed.* **2001**, *40*, 2444. (b) Long, D.-L.; Blake, A. J.; Champness, N. R.; Schröder, M. *Chem. Commun.* **2000**, 2273. (c) Tanase, S.; Andruh, M.; Müller, A.; Schmidtmann, M.; Mathonière, C.; Rombaut, G. *Chem. Commun.* **2001**, 1084. (d) Long, D.-L.; Blake, A. J.; Champness, N. R.; Wilson, C.; Schrder, M. *Chem. Eur. J*. **2002**, *8*, 2026. (e) Ma, B.-Q.; Gao, S.; Sun, H.-L.; Xu, G.-X. *CrystEngComm* **2001**, *35*, 1. (f) Long, D. L.; Blake, A. J.; Champness, N. R.; Wilson, C.; Schroder, M. *J. Am. Chem. Soc.* **2001**, *123*, 3401. (g) Xu, Y.; Yuan, D.; Han, L.; Ma, E.; Wu, M.; Lin, Z.; Hong, M. *Eur. J. Inorg. Chem.* **2005**, 2054. (h) Ma, B.-Q.; Sun, H.-L.; Gao, S. *Inorg. Chem*. **2005**, *44*, 837. (i) Manna, S. C.; Zangrando, E.; Drew, M. G. B.; Ribas, J.; Ray Chaudhuri, N. *Eur. J. Inorg. Chem.* **2006**, 481.

(14) (a) Maji, T. K.; Mostafa, G.; Clemente-Juan, J. M.; Ribas, J.; Lloret, F.; Okamoto, K.; Ray Chaudhuri, N. *Eur. J. Inorg. Chem.* **2003**, 1005 (b) Escuer, A.; Kumar, S. B.; Mautner, F.; Vicente, R. *Inorg. Chim. Acta* **1998**, *269*, 313. (c) Monfort, M.; Bastos, C.; Diaz, C.; Ribas, J. *Inorg. Chim. Acta* **1994**, *218*, 185. (d) Vicente, R.; Escuer, A.; Ribas, J.; Solans, X. *J. Chem. Soc., Dalton Trans.* **1994**, 259. (e) Vicente, R.; Escuer, A.; Penalba, E.; Solans, X.; Font-Bard, Z. M. *Inorg. Chim. Acta* **1997**, *255*, 7.

(15) (a) Maji, T. K.; Sain, S.; Mostafa, G.; Das, D.; Lu, T.H.; Ray Chaudhuri, N. *J. Chem. Soc., Dalton Trans.* **2001**, 3149. (b) Son, S. U.; Kim, B. Y.; Choi, C. H.; Lee, S. W.; Kim, Y. S.; Chung, Y. K. *Chem. Commun.* **2003**, 2528. (c) Karasawa, S.; Zhou, G.; Morikawa, H.; Koga, N. *J. Am. Chem. Soc.* **2003**, *125*, 13676. (d) Uemura, K.; Kitagawa, S.; Fukui, K.; Saito, K. *J. Am. Chem. Soc.* **2004**, *126*, 3817. (e) Huang, Z.; Song, H.-B.; Du, M.; Chen, S. T.; Bu, X.-H.; Ribas, J. *Inorg. Chem.* **2004**, *43*, 931. (f) Shin, D. M.; Lee, I. S.; Chung, Y. K.; Lah, M. S. *Chem. Commun.* **2003**, 1036. (g) Maji, T. K.; Sain, S.; Mostafa, G.; Das, D.; Lu, T. H.; Ray Chaudhuri, N. *J. Chem. Soc., Dalton Trans.* **2001**, 3149.

(16) Sarker, K. K.; Chand, B. G.; Jana, A. D.; Mostafa, G.; Sinha, C. *Inorg. Chim. Acta* **2006**, *359*, 695.

(17) (a) Munakata, M.; Kuroda-Sowa, T.; Maekawa, M.; Hirota, A.; Kitagawa, S.; *Inorg. Chem.* **1995**, *34*, 2705. (b) Bond, A. D.; Haynes, D. A.; Pask, C. M.; Rawson, J. M. *J. Chem. Soc*., *Dalton Trans.* **2002**, 2522. (c) Rovira, C.; Novoa, J. J. *Chem. Eur. J.* **1999**, *5*, 3689.

(18) (a) Fujihara, H.; Yabe, M.; Chiu, J.-J.; Furukawa, N. *Tetrahedron Lett.* **1991**, *32*, 4345. (b) Shima, H.; Furukawa, N. *Tetrahedron* **1995**, *51*, 12239. (c) Ghosh, A. K.; Ghoshal, D.; Drew, M. G. B.; Mostafa, G.; Ray Chaudhuri, N. *Struct. Chem*. **2006**, *17*, 85.

(19) Kabsch, W. *J. Appl. Crystallogr.* **1988**, *21*, 916.

(20) Otwinowski, Z.; Minor, W. *Processing of X-ray Diffraction Data Collected in Oscillation Mode, Methods in Enzymology*; Carter, C. W., Jr.; Sweet, R. M., Eds.; Academic Press: New York, 1997.

(21) (a) Watkin, D. J.; Prout, C. K.; Carruthers, J. R.; Betteridge, P. W. CRYSTALS Issue 10, Chemical Crystallography Laboratory, Oxford-UK, 1996. (b) Single Crystal Structure Analysis Software, Version 3.5.1, Rigaku/MSC, 9009 New Trails Drive, The Woodlands, TX 77381-5209. Rigaku, 3-9-12 Akishima, Tokyo 196-8666, Japan.

(22) SHELX97, Programs for Crystal Structure Analysis (Release 97-2). Sheldrick, G. M. University of Göttingen, Germany, 1998.

(23) (a) Farrugia, L. J.; *J. Appl. Crystallogr.* **1999**, *32*, 837. (b) Spek, A. L. PLATON, Molecular Geometry Program; *J. Appl. Crystallogr*. **2003**, *36*, 7.

(24) Farrugia, L. J. ORTEP-32 for Windows, *J. Appl. Crystallogr*. **1997**, *30*, 565.

(25) (a) Ma, B.-Q.; Gao, S.; Sun, H.-L.; Xu, G.-X. *J. Chem. Soc*., *Dalton Trans.* **2001**, 130. (b) Blake, A. J.; Brett, M. T.; Champness, N. R.; Khlobystov, A. N.; Long, D.-L.; Wilson, C.; Schröder, M. *Chem. Commun.* **2001**, 2258. (c) Tao, J.; Tong, M.-L.; Chen, X.-M.; *J. Chem. Soc*., *Dalton Trans.* **2000**, 3669. (d) Roesky, H. W.; Andruh, M. *Coord. Chem. Rev.* **2003**, *236*, 91. (e) Mantero, D. G.; Neels, A.; Stoeckli-Evans, H. *Inorg. Chem.* **2006**, *45*, 3287.

(26) Nyburg, S. C.; Faerman, C. H *Acta Crystallogr.* **1985**, *B41*, 274.

(27) Etter, M. C.; MacDonald, J. C.; Bernstein, J. *Acta Crystallogr.* **1990**, *B46*, 256.

(28) (a) Bhattacharyya, R.; Pal, D.; Chakrabarti, P. *Protein Eng., Des. Selection* **2004**, *17*, 795−808. (b) Castellano, R. K.; Diederich, F.; Meyer, E. A. *Angew. Chem., Int. Ed.* **2003**, *42*, 1210. (c) Tauer, T. P.; Elizabeth, Derrick, M.; Sherrill, C. D. *J. Phys. Chem. A* **2005**, *109*, 191.

CG060762R